

A directional specific heat study on the gap structure of overdoped $\text{Ba}(\text{Fe}_{1-x}\text{Co}_x)_2\text{As}_2$

Gang Mu,^{1,*} Jun Tang,² Yoichi Tanabe,² Jingtao Xu,² Bin Zeng,³ Bing Shen,³ Fei Han,³ Hai-Hu Wen,^{3,4} Satoshi Heguri,¹ and Katsumi Tanigaki^{1,2,†}

¹*Department of Physics, Graduate School of Science, Tohoku University, Sendai 980-8578, Japan*

²*WPI-AIMR, Tohoku University, Sendai 980-8578, Japan*

³*Institute of Physics and Beijing National Laboratory for Condensed Matter Physics, Chinese Academy of Sciences, P.O. Box 603, Beijing 100190, China*

⁴*National Laboratory for Solid State Microstructures, Department of Physics, Nanjing University, Nanjing 210093, China*

Low-temperature specific heat is measured on the overdoped $\text{Ba}(\text{Fe}_{1-x}\text{Co}_x)_2\text{As}_2$ ($x = 0.13$) single crystal under magnetic fields along different directions. A clear anisotropy is observed on the electronic specific heat coefficient $\gamma(H)$. The value of $\gamma(H)$ is clearly larger with magnetic field along [001] (c -axis) than that within the ab -plane of the crystal lattice, which cannot be attributed to the effect by anisotropy of the upper critical field. Meanwhile, the data show a rather small difference when the direction of the field is rotated from [100] to [110] direction within the ab -plane. Our results suggest that a considerable part of the line nodes is not excited to contribute to the quasiparticle density of states by the field when the field is within the ab -plane. The constraint on the topology of the gap nodes is discussed based on the data.

PACS numbers: 74.20.Rp, 74.70.Xa, 74.62.Dh, 65.40.Ba

The gap structure of the Fe-based superconductors seems to be more complicated than expected, which is found to vary substantially from family to family. The consensus has been reached on several systems, e.g. LaFePO ,^{1,2} KFe_2As_2 ,^{3,4} $\text{BaFe}_2(\text{As}_{1-x}\text{P}_x)_2$,^{5,6} and so on, that nodes exist on the gap structure. However, experimental results gave rather contradicting conclusions on this issue in other systems of the Fe-based superconductors.^{7–18} Furthermore, recent experiments reveal that the gap structure can modulate with the doping concentration even in the same family. In the case of electron-doped (Co- or Ni- doped) 122 system, the increase in the gap anisotropy and even the emergence of gap nodes, as the doping content increases in the overdoped region, are evidenced by many experimental methods.^{17–21} This behavior is attributed to the enhancement of intraband interaction and pair scattering between the electron-like Fermi surfaces as the system is doped away from the optimal point.²²

Specific heat (SH) is one of the most powerful bulk probes for investigating the gap structure of the unconventional superconductors. The variation of electronic SH (C_{el}) versus temperature (T) and magnetic field (H) strongly depends on the gap structures of the superconducting materials. T dependence of C_{el} for a superconductor with line nodes varies as $C_{el} \propto T^2$ in low temperature,^{23,24} while an exponential T dependence is expected for a superconductor with an isotropic gap. In the mixed state, H can induce vortices with a supercurrent flowing perpendicularly to the applied H . The low-energy quasiparticles will undergo a Doppler shift induced by the supercurrent, which can give rise to a considerable enhancement of C_{el} for a nodal superconductor.^{25,26} This is called the Volovik effect. We note here that the Volovik effect is the strongest (weakest) when H is parallel (perpendicular) to the Fermi sur-

face where the nodes reside, because the Doppler shift energy is determined by $\delta E \propto \vec{v}_s \cdot \vec{v}_F$, where \vec{v}_s and \vec{v}_F are the supercurrent velocity and Fermi velocity respectively, and the Volovik effect works mainly at the places near the nodes. This provides valuable information on the topology of the line nodes, when we compare the SH data obtained with H along different directions of the crystal lattice.

A clear evidence for the line nodes in the energy gap has been observed in terms of the T^2 term in C_{el} for the overdoped $\text{Ba}(\text{Fe}_{1-x}\text{Co}_x)_2\text{As}_2$ in our previous studies.²⁰ A quick increase of the electronic SH coefficient $\Delta\gamma(H)$ with H was observed when H was applied in the ab -plane, being consistent with the prediction from the Volovik effect on a nodal superconductor. Meanwhile, the underdoped and optimal doped samples show a small anisotropy on the energy gap. In order to obtain further information on the topology of the line nodes in the overdoped samples, directional SH studies are very warranted. Here we report such important experiments. The unambiguous anisotropic behaviors related to the Volovik effect imposed on line nodes can be confirmed by the fact that the electronic SH coefficient $\gamma(H)$ increases more quickly when H is parallel to the c -axis than that within the ab -plane. The possible constraint on the topology of line nodes is discussed based on the observations.

The $\text{Ba}(\text{Fe}_{1-x}\text{Co}_x)_2\text{As}_2$ single crystals were grown by a self-flux method. As-grown samples were annealed under high vacuum at 800 °C for 20 days. The dc magnetization measurements were made with a superconducting quantum interference device (Quantum Design, MPMS). SH was measured with H along three directions (see inset (b) of Fig. 1). The data obtained with H within ab -plane were collected with a Helium-3 system attached with the physical property measurement system (Quantum Design, PPMS), while those with H along c -axis

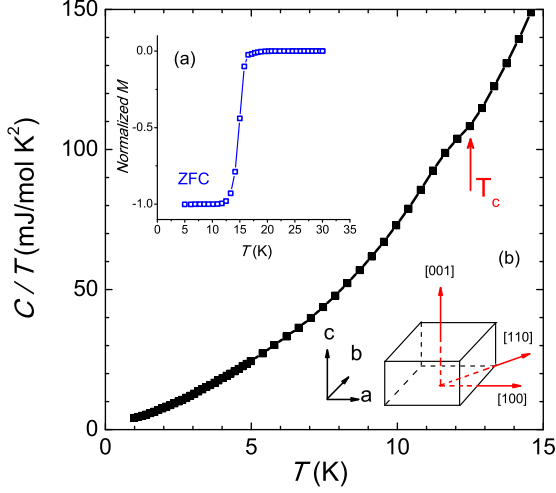


FIG. 1: (color online) Main frame: temperature dependence of SH coefficient (C/T) for the overdoped $\text{Ba}(\text{Fe}_{1-x}\text{Co}_x)_2\text{As}_2$ with $x = 0.13$ under zero field. Inset (a): diamagnetic transition of the same sample. Inset (b): schematic representation of three directions along which the magnetic field is applied.

were obtained in a standard mode.

The superconducting transition of the selected sample with $x = 0.13$ is checked by the dc magnetization and specific heat measurements. The present sample was determined to be in the overdoped region of the phase diagram.²⁰ In Fig. 1, we show the T dependence of the SH coefficient C/T up to 15 K under zero field. The kink at about 12.5 K indicated by red arrow is the superconducting transition. This temperature corresponds to the end point of the diamagnetic transition, as shown in the inset (a) of Fig. 1.

We measured SH of $\text{Ba}(\text{Fe}_{1-x}\text{Co}_x)_2\text{As}_2$ with $x = 0.13$ under H along the [100], [110], and [001] directions of the crystal lattice. A schematic representation of the three directions is given in inset (b) of Fig. 1. The raw data of SH under H of these three directions are plotted as C/T vs T^2 in Figs. 2(a)-(c), respectively. Here we focus on the behaviors of our data in the low- T region below 4.5 K. One can see that the behaviors of the data with H along [100] and [110] directions are quite similar with each other. While the data with H along the [001] direction increase more quickly with H . Nevertheless, all the three sets of data show clear negative curvatures in the T range we studied. In our previous work,²⁰ we have attributed this behavior to the presence of the T^2 term in the electronic SH, which is consistent with the prediction for the superconductors with line nodes in the energy gap. The data were then fitted by the following equation

$$C(T, H) = \gamma(H)T + \alpha(H)T^2 + \beta T^3, \quad (1)$$

where $\gamma(H)$ is the electronic SH coefficient under H , $\alpha(H)$ is the coefficient of the T^2 term under H , and β is

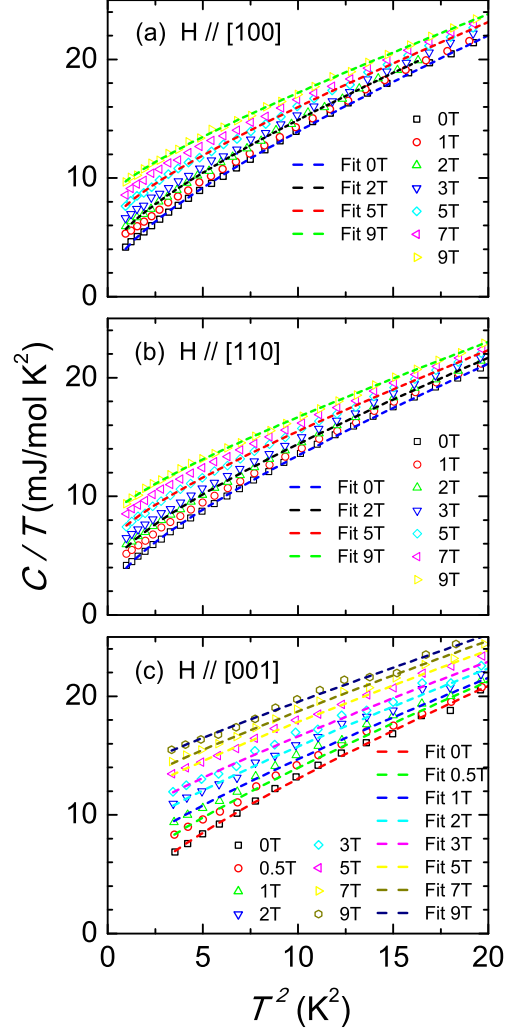


FIG. 2: (color online) Raw SH data of the $\text{Ba}(\text{Fe}_{1-x}\text{Co}_x)_2\text{As}_2$ sample with $x = 0.13$ under fields aligned with the [100], [110], and [001] directions of the crystal lattice, respectively. The dashed lines represent the results of theoretical fitting.

the phonon SH coefficient. The value of β was found to be almost independent of H . Consequently, here we average the value of β under different fields and fix it when fitting the data using Eq. (1). The effect of small fluctuations of β is transferred to the error bar of the resulting fitting parameters $\gamma(H)$ and $\alpha(H)$ (see Fig. 3). The fitting results are displayed by the dashed lines in Fig. 2. Only four selected fitting curves are shown in Figs. 2(a) and (b) respectively for clarity. It is clear that these curves describe the negative-curvature features commendably.

The fitting parameters $\gamma(H)$ and $\alpha(H)$ are shown in Figs. 3(a) and (b). The horizontal ordinate is normalized with the upper critical field H_{c2} , so as to eliminate the effect of anisotropy of H_{c2} on the H dependent data. As we have stated,²⁰ H_{c2} within the ab -plane is about 28 T, from which the H_{c2} value along the c -axis can be esti-

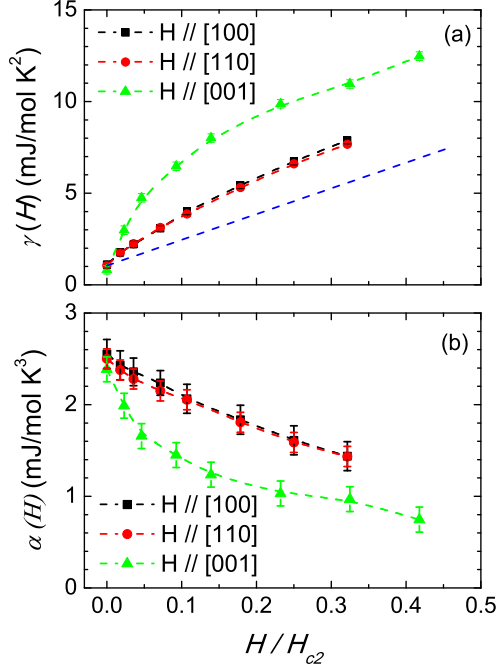


FIG. 3: (color online) Field dependence of $\gamma(H)$ and $\alpha(H)$ with H along three directions. H is normalized with the upper critical field H_{c2} . The blue dashed line in (a) shows the theoretical curve for the case with an isotropic gap.

mated using the its anisotropy ($\Gamma \equiv H_{c2}^{ab}/H_{c2}^c$). From the reported high- H experiments, we know that Γ decreases when reducing T and finally reaches about 1.1 at 0.7 K for the near-optimal doped $\text{Ba}(\text{Fe}_{1-x}\text{Co}_x)_2\text{As}_2$.^{27,28} Here we take the value $\Gamma \sim 1.3$ for the present overdoped case, which would be no less than the actual value. Such a treatment will not affect the conclusions described below, because a smaller Γ would result in the enhancement of the anisotropic features.

Both $\gamma(H)$ and $\alpha(H)$ show small deviations among the three directions when H is approaching zero, which confirms the reliability of our data even though the data with H along c -axis is only measured down to 1.9 K. From Fig. 3(a) one can see that all the three sets of data are clearly above the blue dashed line, which represents the theoretical curve for the case with an isotropic gap. This is consistent with the features induced by the Volovik effect in a nodal superconductor. It is clear that $\gamma(H)$ with H aligned with c -axis (hereafter abbreviated as $\gamma^c(H)$) increases more quickly than that within the ab -plane (abbreviated as $\gamma^{ab}(H)$). We found that $\gamma^{ab}(H)$ takes up about 70% of $\gamma^c(H)$ when the reduced H/H_{c2} equals to 0.3. In sharp contrast, the data within the ab -plane remain almost unchanged within the extent of error bar when H is rotated from [100] to [110] direction. Considering the fact that the increase of $\gamma(H)$ is induced by Volovik effect, our present observations suggest that the Volovik effect is stronger when H is applied along the

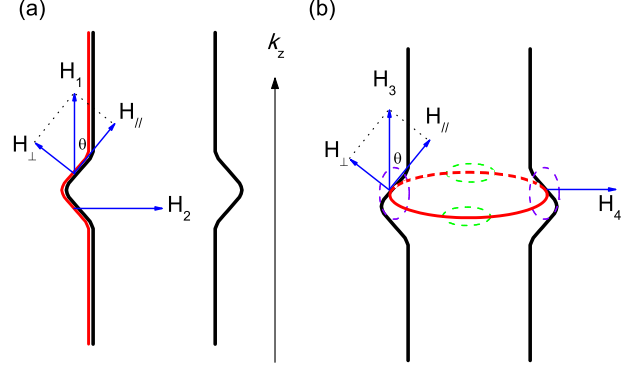


FIG. 4: (color online) Schematic diagram of two typical models of line nodes on one of the Fermi surfaces with a 3D character. Here we only display a longitudinal section of the Fermi surface shown by the two black lines. The vertical (a) and horizontal (b) line nodes are shown by the red lines.

c -axis than that within the ab -plane. The anisotropic features of H dependent $\alpha(H)$ shown in Fig. 3(b) also support such an argument because the decrease of $\alpha(H)$ is associated with the Volovik effect. Obviously, these findings will provide a hint for investigating the topology of the nodes, which will be discussed in the following.

Different topologies of the nodes or gap minima have been proposed and the significant influence by the three-dimensional (3D) features of the Fermi surface (FS) has been noticed, by both experiments and calculations.^{17,18,29,30} Consequently, here we consider the constraint by our data on the line nodes based on the two typical models, where the line nodes with two different orientations are proposed on one of the FSs with a 3D character. As shown in Fig. 4, the longitudinal section of the FS is shown by two black lines. The red line in Fig. 4(a) and red circle in Fig. 4(b) represent the positions of vertical and horizontal line nodes, respectively.

We first check the situation of the vertical-node case as shown in Fig. 4(a). When H is applied parallel to k_z , which is shown by the blue arrow H_1 , the segments of line nodes on the FS with no or small 3D features will experience a strong Volovik effect, while that with clear 3D features only undergo a depressed Volovik effect induced by the projection of H on the tangent surface ($H_{\parallel} = H_1 \cos \theta$), where angle θ describes the deviation of the FS from the direction of k_z . When H is perpendicular to k_z , the situation will be rather complex because the direction can be rotated by 360° . The Volovik effect is the weakest if H is rotated to the nodal direction (see H_2 in Fig. 4(a)) because only the segments of nodes on the 3D-dispersed FS can experience the Volovik effect with a projected field $H_{\parallel} = H_2 \sin \theta$. The situations with H along other directions may vary depending on the number of the vertical line nodes and their distribution on the FS. Nevertheless, the clear anisotropy between $\gamma^c(H)$ and

$\gamma^{ab}(H)$ requires that the angle θ or the proportion of the 3D-dispersed FS should not be too large.

One problem in the scenario described above is that $\gamma^{ab}(H)$ should show some variation in principle when H is rotated within ab -plane, which was not observed in our data. One possibility is that the number of nodes is large (e.g. larger than 4), so that the variation will be weakened. Another explanation may be given by calculations based on an extended-s-wave case,³¹ where an attenuation of the SH vibration is predicted because of the elliptical FS pockets near the M points. Although both cases do not support the d -wave symmetry of the energy gap, we can't rule out the possibility that both [100] and [110] directions deviate from the nodal direction, and consequently we failed to observe the difference between the two directions. This may need further clarification by detailed angle-resolved SH measurements.

The situation becomes somewhat different if we have the horizontal line nodes, as shown in Fig. 4(b). When H is parallel to k_z (see H_3), the whole nodal line will experience a depressed Volovik effect induced by $H_{\parallel} = H_3 \cos \theta$. Whereas when H is applied perpendicular to k_z (see H_4), the segments of nodes on the areas of the FS marked by the green circles will experience a strong Volovik effect because H is roughly parallel to these parts of FS. Meanwhile, the segments of nodes marked by the violet circles will experience a depressed Volovik effect induced by $H_{\parallel} = H_4 \sin \theta$. The fact that $\gamma^c(H)$ is clearly larger than $\gamma^{ab}(H)$ in our data means that the overall Volovik effect when H is parallel to k_z should exceed that with H perpendicular to k_z . This implies that the angle θ cannot be too large. The advantage of this latter model is that the unobservable vibration of $\gamma^{ab}(H)$ can be ex-

plained naturally. A recent angle resolved photoemission spectroscopy (ARPES) study on $\text{BaFe}_2(\text{As}_{0.7}\text{P}_{0.3})_2$ has revealed such a horizontal circular line node on the hole FS around the Z point at the Brillouin zone boundary.³²

In summary, we studied the low-temperature SH on the overdoped $\text{Ba}(\text{Fe}_{1-x}\text{Co}_x)_2\text{As}_2$ with H along three different directions. Clear anisotropic behaviors are observed from H dependent data. The electronic SH coefficient $\gamma(H)$ increases more quickly when H is in the c -axis direction than that within the ab -plane, whereas the data remain unchanged within our resolution when H is rotated within the ab -plane. Our results suggest that a considerable portion of the line nodes is not excited plenarily to contribute to the density of states when H is in the ab in-plane. These conclusions supply an important constraint when investigating the topologies of the line nodes in this system.

Acknowledgments

We acknowledge discussions with Dr. Yue Wang. The research is partially supported by Scientific Research on Priority Areas of New Materials Science Using Regulated Nano Spaces, the Ministry of Education, Science, Sports and Culture, Grant-in-Aid for Science, and Technology of Japan. The work is partially supported by Tohoku GCOE Program and by the approval of the Japan Synchrotron Radiation Research Institute (JASRI). G M expresses special thanks to Grants-in-Aid for Scientific Research from the Japan Society for the Promotion of Science (JSPS) (Grant No. P10026).

* mugang@sspns.phys.tohoku.ac.jp

† tanigaki@sspns.phys.tohoku.ac.jp

¹ J. D. Fletcher, A. Serafin, L. Malone, J. G. Analytis, J. H. Chu, A. S. Erickson, I. R. Fisher, and A. Carrington, *Phys. Rev. Lett.* **102**, 147001 (2009).

² C. W. Hicks, T. M. Lippman, M. E. Huber, J. G. Analytis, J. H. Chu, A. S. Erickson, I. R. Fisher, and K. A. Moler, *Phys. Rev. Lett.* **103**, 127003 (2009).

³ J. K. Dong, S. Y. Zhou, T. Y. Guan, H. Zhang, Y. F. Dai, X. Qiu, X. F. Wang, Y. He, X. H. Chen, and S. Y. Li, *Phys. Rev. Lett.* **104**, 087005 (2010).

⁴ H. Fukazawa, Y. Yamada, K. Kondo, T. Saito, Y. Kohori, K. Kuga, Y. Matsumoto, S. Nakatsuji, H. Kito, P. M. Shirage, K. Kihou, N. Takeshita, C. H. Lee, A. Iyo, and H. Eisaki, *J. Phys. Soc. Jpn.* **78**, 083712 (2009).

⁵ M. Yamashita, Y. Senshu, T. Shibauchi, S. Kasahara, K. Hashimoto, D. Watanabe, H. Ikeda, T. Terashima, I. Vekhter, A. B. Vorontsov, Y. Matsuda, arXiv: 1103.0885 (2011).

⁶ T. Dulguun, H. Mukuda, H. Kinouchi, M. Yashima, Y. Kitaoka, T. Kobayashi, S. Miyasaka, S. Tajima, arXiv: 1108.4480 (2011).

⁷ G. Mu, X. Zhu, L. Fang, L. Shan, C. Ren, and H. H. Wen,

Chin. Phys. Lett. **25**, 2221 (2008).

⁸ T. Y. Chen, Z. Tesanovic, R. H. Liu, X. H. Chen, and C. L. Chien, *Nature (London)* **453**, 1224 (2008).

⁹ H. Ding, P. Richard, K. Nakayama, K. Sugawara, T. Arakane, Y. Sekiba, A. Takayama, S. Souma, T. Sato, T. Takahashi, Z. Wang, X. Dai, Z. Fang, G. F. Chen, J. L. Luo, and N. L. Wang, *Europhys. Lett.* **83**, 47001 (2008).

¹⁰ K. Hashimoto, T. Shibauchi, T. Kato, K. Ikada, R. Okazaki, H. Shishido, M. Ishikado, H. Kito, A. Iyo, H. Eisaki, S. Shamoto, and Y. Matsuda, *Phys. Rev. Lett.* **102**, 017002 (2009).

¹¹ C. Ren, Z. S. Wang, H. Q. Luo, H. Yang, L. Shan, and H. H. Wen, *Phys. Rev. Lett.* **101**, 257006 (2008).

¹² G. Mu, H. Q. Luo, Z. S. Wang, L. Shan, C. Ren, and H. H. Wen, *Phys. Rev. B* **79**, 174501 (2009).

¹³ J. P. Reid, M. A. Tanatar, X. G. Luo, H. Shakeripour, S. R. de Cotret, N. D. Leyraud, J. Chang, B. Shen, H.-H. Wen, H. Kim, R. Prozorov, L. Taillefer, arXiv: 1105.2232 (2011).

¹⁴ B. Zeng, G. Mu, H. Q. Luo, T. Xiang, I. I. Mazin, H. Yang, L. Shan, C. Ren, P. C. Dai, and H. H. Wen, *Nat. Commun.* **1**, 112 (2010).

¹⁵ H. Miao, P. Richard, Y. Tanaka, K. Nakayama, T. Qian,

- K. Umezawa, T. Sato, Y.-M. Xu, Y.-B. Shi, N. Xu, X.-P. Wang, P. Zhang, H.-B. Yang, Z.-J. Xu, J. S. Wen, G.-D. Gu, X. Dai, J.-P. Hu, T. Takahashi, and H. Ding, arXiv:1107.0985 (2011).
- ¹⁶ C. L. Song, Y. L. Wang, P. Cheng, Y. P. Jiang, W. Li, T. Zhang, Z. Li, K. He, L. L. Wang, J. F. Jia, H. H. Hung, C. J. Wu, X. C. Ma, X. Chen, and Q. K. Xue, *Science* **332**, 1410 (2010).
- ¹⁷ C. Martin, H. Kim, R. T. Gordon, N. Ni, V. G. Kogan, S. L. Budko, P. C. Canfield, M. A. Tanatar, and R. Prozorov, *Phys. Rev. B* **81**, 060505(R) (2010).
- ¹⁸ J. P. Reid, M. A. Tanatar, X. G. Luo, H. Shakeripour, N. Doiron-Leyraud, N. Ni, S. L. Bud'ko, P. C. Canfield, R. Prozorov, and L. Taillefer, *Phys. Rev. B* **82**, 064501 (2010).
- ¹⁹ K. Gofryk, A. B. Vorontsov, I. Vekhter, A. S. Sefat, T. Imai, E. D. Bauer, J. D. Thompson, and F. Ronning, *Phys. Rev. B* **83**, 064513 (2011).
- ²⁰ G. Mu, J. Tang, Y. Tanabe, J. T. Xu, S. Heguri, and K. Tanigaki, *Phys. Rev. B* **84**, 054505 (2011).
- ²¹ C. Ren, Z. S. Wang, Z. Y. Wang, H. Q. Luo, X. Y. Lu, B. Sheng, C. H. Li, L. Shan, H. Yang, and H. H. Wen, e-print arXiv:1106.2891 (2011).
- ²² P. J. Hirschfeld, M. M. Korshunov, I. I. Mazin, arXiv:1106.3712 (2011).
- ²³ M. Sigrist and K. Ueda, *Rev. Mod. Phys.* **63**, 239 (1991).
- ²⁴ N. E. Hussey, *Advances in Physics*, **51**, 1685 (2002).
- ²⁵ G. E. Volovik, *JETP Lett.* **58**, 469 (1993).
- ²⁶ G. E. Volovik, *JETP Lett.* **65**, 491 (1997).
- ²⁷ M. Kano, Y. Kohama, D. Graf, F. Balakirev, A. S. Sefat, M. A. McGuire, B. C. Sales, D. Mandrus, and S. W. Tozer, *J. Phys. Soc. Jpn.* **78**, 084719 (2009).
- ²⁸ A. Yamamoto, J. Jaroszynski, C. Tarantini, L. Balicas, J. Jiang, A. Gurevich, D. C. Larbalestier, R. Jin, A. S. Sefat, M. A. McGuire, B. C. Sales, D. K. Christen, and D. Mandrus, *Appl. Phys. Lett.* **94**, 062511 (2009).
- ²⁹ S. Graser, A. F. Kemper, T. A. Maier, H.-P. Cheng, P. J. Hirschfeld, and D. J. Scalapino, *Phys. Rev. B* **81**, 214503 (2010).
- ³⁰ K. Suzuki, H. Usui, and K. Kuroki, *J. Phys. Soc. Jpn.* **80**, 013710 (2011).
- ³¹ S. Graser, G. R. Boyd, C. Cao, H. P. Cheng, P. J. Hirschfeld, and D. J. Scalapino, *Phys. Rev. B* **77**, 180514(R) (2008).
- ³² Y. Zhang, Z. R. Ye, Q. Q. Ge, F. Chen, J. Jiang, M. Xu, B. P. Xie, and D. L. Feng, e-print arXiv:1109.0229 (2011).